Materials Science in Semiconductor Processing 60 (2017) 1–4

Contents lists available at ScienceDirect

Materials Science in Semiconductor Processing

journal homepage: www.elsevier.com/locate/mssp

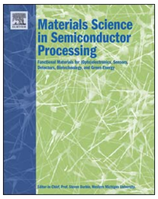

Short communication

Organic thin-film transistors with bilayer of rubbed and evaporated hydrocarbon-based acene as active layer

Shunpei Funada, Safizan Shaari, Shigeki Naka, Hiroyuki Okada*

Graduate School of Science and Engineering, University of Toyama, 3190 Gofuku, Toyama 930-8555, Japan

ARTICLE INFO

Keywords:
Organic transistor

ABSTRACT

We have investigated organic thin-film transistors (OTFTs) with a bilayer of rubbed and evaporated hydrocarbon-based acene 2,7-dioctyl[1]benzothieno[3,2-b][1]benzothiophene (C8-BTBT) as an active layer. Using a rubbing process after spin-coating the C8-BTBT, crystallinity of the C8-BTBT thin film was improved and resultant superior OTFT characteristics were realized. We obtained a field-effect mobility of 1.6 cm^2/Vs, a threshold voltage of −8.2 V, an on-off ratio of 10^6, and a subthreshold swing of 55 mV/decade.

1. Introduction

Organic thin-film transistors (OTFTs) [1–6] have been attracting interest for use in large-area electronic applications, such as electronic papers [7,8], flexible organic light-emitting diode displays [9,10], and radio frequency identification tags [11]. In the context of flexible electronics applications, OTFTs are highly desirable because of their flexibility and their maximum process temperature of as high as 150 °C. Organic materials can be classified into small-molecule systems and polymer systems. In the initial stage of OTFT research, mobility exceeding 1 cm^2/Vs was reported using the small organic molecule of pentacene with SiO_2 as an insulator [1–6]. A higher mobility can be achieved using a dendrite structure with steps of single-molecule length and a micron-scale polycrystalline grain structure. In the last twenty years, organic material systems have made tremendous progress. In terms of the organic materials, hydrocarbon-based acenes, such as 2,7-dioctyl[1]benzothieno[3,2-b][1]benzothiophene (C8-BTBT), have consistently shown excellent carrier mobility and high stability [12,13]. A higher-ordered c-axis alignment and a large planar terrace structure in the in-plane direction have been obtained using hydrocarbon-based acenes. However, such acenes have several issues in terms of the polycrystalline grains of OTFTs, deviation of the in-plane direction of individual crystals, and the uncontrollability of grain boundaries. Furthermore, the width and potential barrier height of the interfacial state could not be controlled and the device performances in terms of mobility and threshold voltage varied widely. To resolve these issues, many researchers have studied the fabrication of OTFTs via the solubilization of alkyl chains into molecular structures [13]. Spin-coated pentacene OTFTs have organic films with an extremely large grain size and produce a consistent mobility compared with OTFTs fabricated using the conventional evaporation process [14]. Many key techniques for controlling the direction of crystal growth and ensuring a slow crystallization process have been reported [15–19]. A rubbing method was also reported to control the crystal growth of devices with a liquid-crystalline polymer semiconductor [15,16]. Moreover, lower variations of mobility and threshold voltage were reported using a flow-coating method with 6,13-Bis (triisopropylsilylethynyl) (TIPS) pentacene [17]. For controlling the drying direction, a crystal growth method using a perpendicular glass piece was proposed [18]. Furthermore, a technique combining antisolvent crystallization with inkjet printing to produce organic semiconducting thin films of high crystallinity that grow at liquid–air interfaces was proposed [19].

In this study, we have investigated OTFTs that employ a bilayer of rubbed and evaporated C8-BTBT as an active layer to improve the crystal growth and device characteristics.

2. Experiment

Fig. 1 shows the fabrication process of the bilayer OTFT structure under study. A heavily doped n-type Si wafer was used as a substrate, which had a silicon dioxide (SiO_2) layer with a thickness of 1000 Å. The Si wafer was consecutively cleaned by ultrasonic cleaning with acetone, isopropanol, and deionized (DI) water. Then, 0.75 wt% C8-BTBT (chloroform) solution was spin-coated on the substrate (Fig. 1(a)). Here, thickness of the spin-coated C8-BTBT was 480 Å. Next, a rubbing process parallel to the current flow was carried out. Cross-sectional view of the rubbing process are shown in Fig. 2. Rubbing roller is rotated to the rotation direction of curved arrow. At the same time, a

---

* Corresponding author.
E-mail address: okada@eng.u-toyama.ac.jp (H. Okada).

http://dx.doi.org/10.1016/j.mssp.2016.12.020
Received 2 August 2016; Received in revised form 17 October 2016; Accepted 18 December 2016

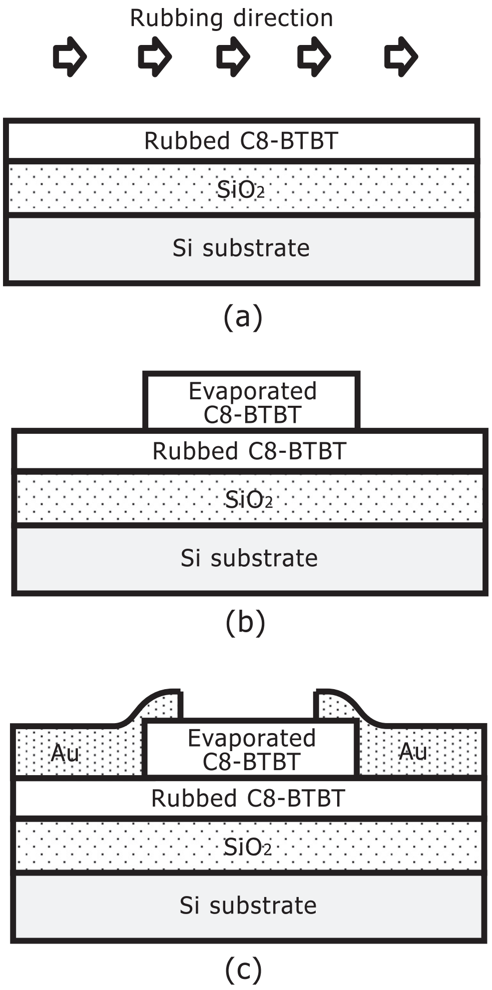

Fig. 1. Fabrication process of bilayer OTFT under study. (a) C8-BTBT spin-coating & rubbing, (b) C8-BTBT evaporation, and (c) gold evaporation.

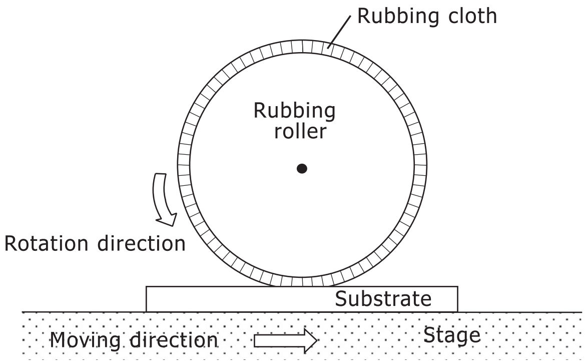

Fig. 2. Cross-sectional view of rubbing process. Rubbing cloth is touched to substrate and fiber of cloth is deformed on top of substrate.

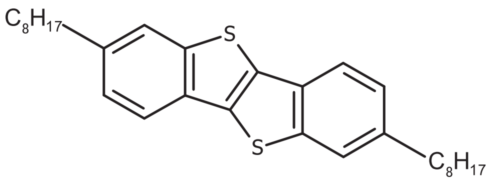

Fig. 3. Molecular structure of C8-BTBT.

stage is slowly moved to the moving direction of straight arrow. The rubbing direction is defined as the rotation direction, as shown in Figs. 1(a) and 2. In this situation, only a fiber of the cloth is touched to the surface of substrate. Subsequently, a 600-Å-thick layer of C8-BTBT was evaporated (Fig. 1(b)). Fig. 3 shows the molecular structure of C8-BTBT. Finally, gold source and drain electrodes with a thickness of 550 Å were evaporated, where, the thickness was monitored using quartz crystal microbalances. The top-contact OTFT structure shown in Fig. 1(c) was fabricated, where the channel length and width were 1.5 mm and 1 mm, respectively. The long channel length was used to reduce the series resistance effect. A metal shadow mask was placed on the substrate during evaporation to pattern the C8-BTBT active layer and the source/drain electrodes. The evaporation rates of the organic semiconductor and the gold were 0.2 Å/s and 0.5 Å/s, respectively. X-ray diffraction (XRD) analysis (Bruker AXS, D8 DISCOVER) and field emission scanning electron microscopy (FE-SEM) analysis (JEOL, JSM-6700F) were carried out in order to evaluate quality of c-axis orientation and surface conformation, respectively, for C8-BTBT thin film. After fabricating the device structure, the drain voltage (V_D) vs drain current (I_D) and gate voltage (V_G) vs I_D characteristics were measured using a semiconductor parameter analyzer (HP4144B). A mobility, a threshold voltage and an offset voltage were estimated by fitting an ideal V_D-I_D characteristics [20].

3. Results and discussions

Before starting an evaluation of OTFT characteristics, a film quality of the C8-BTBT thin film is evaluated using XRD analysis. Fig. 4 shows XRD results of the C8-BTBT thin films with various fabrication process, after spin-coating (a), after spin-coating with rubbing process (b), after second layer evaporation (c), and after second layer evaporation on rubbed C8-BTBT thin film (d). Where, diffraction peaks of (001), (002), and (003) plane were observed in each pattern. Resultant *d*-spacing was around 28.6 Å, which is identical to the reported data of *d*-spacing in the C8-BTBT thin film [13]. After rubbing process, the X-ray peak intensity was dramatically increased, as compared to (a) and (b), where peak intensity of (001) plane was 28,760 cps and 52,450 cps, respectively. By evaporating the second C8-BTBT layer, the peak intensity was also increased, as shown in Fig. 4(c) and (d), where, peak intensity of (001) was 81,180 cps and 98,060 cps, respectively. As a result, the crystallinity of the organic film is improved by rubbing process and additional C8-BTBT layer evaporation.

Fig. 5 shows FE-SEM images of the C8-BTBT thin films without rubbing (Fig. 5(a)) and with rubbing condition (Fig. 5(b)) after second layer evaporation. Without rubbing condition, relatively flat, several-μm-sized and randomly-oriented polycrystalline domains are observed. There are small defect spots with size of several-hundred nm between grain boundaries, where, the number of defect spots per area was 52 μm^{-2}. With rubbing condition, crystalline structure was dramati-

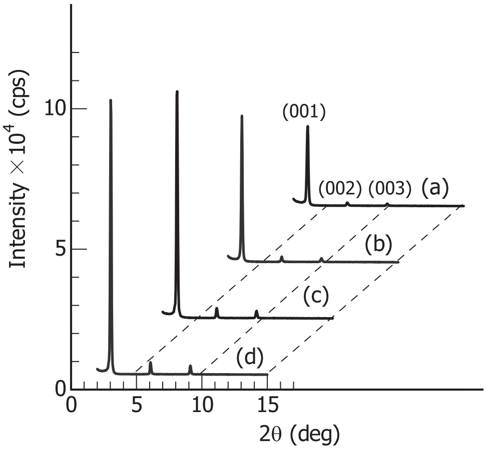

Fig. 4. X-ray diffraction patterns of C8-BTBT with various fabrication process. (a) After spin-coating, (b) after spin-coating with rubbing process, (c) after second layer evaporation, and (d) after second layer evaporation on rubbed C8-BTBT thin film.